

RESEARCH ARTICLE

Zinc transporter ZIP13 suppresses beige adipocyte biogenesis and energy expenditure by regulating C/EBP- β expression

Ayako Fukunaka^{1,2,3}, Toshiyuki Fukada^{4,5,6}, Jinhyuk Bhin⁷, Luka Suzuki¹, Takamasa Tsuzuki⁸, Yuri Takamine⁹, Bum-Ho Bin⁵, Toshinori Yoshihara⁸, Noriko Ichinoseki-Sekine⁸, Hisashi Naito⁸, Takeshi Miyatsuka¹, Shinzaburo Takamiya⁹, Tsutomu Sasaki¹⁰, Takeshi Inagaki¹¹, Tadahiro Kitamura¹⁰, Shingo Kajimura^{12,13}, Hirotaka Watada^{1,14,15,16}, Yoshio Fujitani^{1,2,3,16*}



1 Department of Metabolism & Endocrinology, Juntendo University Graduate School of Medicine, Tokyo, Japan, **2** Laboratory of Developmental Biology & Metabolism, Institute for Molecular & Cellular Regulation, Gunma University, Maebashi, Gunma, Japan, **3** AMED-JST-CREST Program, Tokyo, Japan, **4** Faculty of Pharmaceutical Sciences, Tokushima Bunri University, Tokushima, Japan, **5** Division of Pathology, Department of Oral Diagnostic Sciences, School of Dentistry, Showa University, Tokyo, Japan, **6** RIKEN Center for Integrative Medical Sciences, Yokohama, Japan, **7** Department of Molecular Carcinogenesis, The Netherlands Cancer Institute, Amsterdam, The Netherlands, **8** Graduate School of Health and Sports Science, Juntendo University, Inzai, Chiba, Japan, **9** Department of Tropical Medicine and Parasitology, Graduate School of Medicine, Juntendo University, Tokyo, Japan, **10** Laboratory of Metabolic Signaling, Institute for Molecular & Cellular Regulation, Gunma University, Maebashi, Gunma, Japan, **11** Laboratory of Epigenetics and Metabolism, Institute for Molecular & Cellular Regulation, Gunma University, Maebashi, Gunma, Japan, **12** UCSF Diabetes Center and Department of Cell and Tissue Biology, University of California—San Francisco, San Francisco, United States of America, **13** PRESTO-JST, Tokyo, Japan, **14** Center for Identification of Diabetic Therapeutic Targets, Juntendo University Graduate School of Medicine, Tokyo, Japan, **15** Sportology Center, Juntendo University Graduate School of Medicine, Tokyo, Japan, **16** Center for Therapeutic Innovations in Diabetes, Juntendo University Graduate School of Medicine, Tokyo, Japan

* fujitani@gunma-u.ac.jp

OPEN ACCESS

Citation: Fukunaka A, Fukada T, Bhin J, Suzuki L, Tsuzuki T, Takamine Y, et al. (2017) Zinc transporter ZIP13 suppresses beige adipocyte biogenesis and energy expenditure by regulating C/EBP- β expression. *PLoS Genet* 13(8): e1006950. <https://doi.org/10.1371/journal.pgen.1006950>

Editor: Gregory S. Barsh, Stanford University School of Medicine, UNITED STATES

Received: October 6, 2016

Accepted: July 31, 2017

Published: August 30, 2017

Copyright: © 2017 Fukunaka et al. This is an open access article distributed under the terms of the [Creative Commons Attribution License](https://creativecommons.org/licenses/by/4.0/), which permits unrestricted use, distribution, and reproduction in any medium, provided the original author and source are credited.

Data Availability Statement: The gene expression data set was deposited in the Gene Expression Omnibus database (GSE77933).

Funding: This work was supported by grants from the Ministry of Education, Culture, Sports, Science and Technology of Japan (to AF (16K09764, 26860700, 24790936), YF (25461364), and TF (17H04011)), Fumi Yamamura Memorial Foundation for Female Natural Scientists, Suzuken Memorial Foundation, Banyu Life Science Foundation International, Front Runner of Future

Abstract

Given the relevance of beige adipocytes in adult humans, a better understanding of the molecular circuits involved in beige adipocyte biogenesis has provided new insight into human brown adipocyte biology. Genetic mutations in *SLC39A13/ZIP13*, a member of zinc transporter family, are known to reduce adipose tissue mass in humans; however, the underlying mechanisms remains unknown. Here, we demonstrate that the *Zip13*-deficient mouse shows enhanced beige adipocyte biogenesis and energy expenditure, and shows ameliorated diet-induced obesity and insulin resistance. Both gain- and loss-of-function studies showed that an accumulation of the CCAAT/enhancer binding protein- β (C/EBP- β) protein, which cooperates with dominant transcriptional co-regulator PR domain containing 16 (PRDM16) to determine brown/beige adipocyte lineage, is essential for the enhanced adipocyte browning caused by the loss of ZIP13. Furthermore, ZIP13-mediated zinc transport is a prerequisite for degrading the C/EBP- β protein to inhibit adipocyte browning. Thus, our data reveal an unexpected association between zinc homeostasis and beige adipocyte biogenesis, which may contribute significantly to the development of new therapies for obesity and metabolic syndrome.

Diabetes Research, Astellas Foundation of Research on Metabolic Disorders, and Japan Diabetes Foundation (to AF). This work was supported by the Vehicle Racing Commemorative Foundation (to TF). This research is supported by the Program for Promoting Practical Applications of Genomic Medicine from Japan Agency for Medical Research and development, AMED (to HW). The funders had no role in study design, data collection and analysis, decision to publish, or preparation of the manuscript.

Competing interests: I have read the journal's policy and the authors of this manuscript have the following competing interests: HW has received lecture fees from Daiichi Sankyo Co. Ltd., (Daiichi Sankyo), Takeda Pharmaceutical Co. Ltd. (Takeda), MSD, Sanofi, Ono Pharmaceutical Co. Ltd. (Ono), Novartis Pharma K.K. (Novartis), Astellas Pharma, Inc. (Astellas), Sumitomo Dainippon Pharma Co. Ltd. (Sumitomo Dainippon), Mitsubishi Tanabe Pharma Corporation (Mitsubishi Tanabe), Novo Nordisk Pharma Ltd. (Novo Nordisk), and Sanwa Kagaku Kenkyusho Co. Ltd. (Sanwa Kagaku), and research funding from Sanofi, Novo Nordisk, Novartis, AstraZeneca, Sanwa Kagaku, Ono, MSD, Boehringer Ingelheim, Kissei Pharmaceutical Co. Ltd., Takeda, Daiichi Sankyo, and Eli Lilly & Co. (Eli Lilly).

Author summary

Inducible brown fat-like cells, named beige adipocytes have recently been a topic of great interest, mainly because they are induced in response to external cues, and are closely associated with adult human brown adipocyte. Therefore, the identification of selective molecular circuits involved in beige adipocyte biogenesis and thermogenesis will enable the selective induction of white adipocyte browning as a therapy for obesity. Here, we show that zinc homeostasis, which is controlled by ZIP13, a protein associated with human disease, is essential for the accurate regulation of beige adipocyte differentiation. Inhibition of ZIP13 function enhances beige adipocyte biogenesis and thermogenesis, highlighting the potential of ZIP13 as a therapeutic target for obesity and metabolic syndrome.

Introduction

Obesity and its associated metabolic diseases are caused by a long-term imbalance between energy intake and energy expenditure. Adipose tissue, a major factor in controlling the balance of energy, is composed of white and brown adipocytes, which have two distinct functions: white adipocytes store excess energy, whereas brown adipocytes specialize in expending energy. The unique metabolic properties of brown adipocytes depend on their mitochondrial density, fuel oxidation capacity, and exclusive expression of uncoupling protein-1 (UCP1). Inducible brown fat-like cells, named beige adipocytes, have also been identified in white adipose tissue (WAT). Beige adipocytes are induced by various external cues, such as chronic cold exposure, long-term treatment with a peroxisome proliferator-activated receptor (PPAR)- γ agonist, cancer cachexia, and bariatric surgery [1–3]. The presence and activity of thermogenic adipocytes (brown and beige adipocytes) are associated with improved global metabolic fitness, such as improvements in insulin resistance and glucose homeostasis [2,4,5]; conversely, thermogenic adipocytes decrease with age and obesity in mice and humans [6,7]. Recent studies indicate that adult human brown adipose tissue (BAT) in the supraclavicular region has beige-like characteristics [8–11]. These findings indicate the potential importance of beige fats in human obesity and metabolic disease. Therefore, identifying a selective molecular pathway that regulates the acquisition of beige adipocyte properties will enable us to selectively and preferentially promote beige adipocyte biogenesis and thermogenesis as a therapy for obese or older subjects who do not have active BAT depots [1].

Identifying and implementing therapies based on beige fat requires a detailed understanding of the differences in the developmental mechanisms and functions of white, brown, and beige adipocytes. Differentiation mechanisms of all of these fat cell types share many transcriptional regulators, such as PPAR γ and members of the CCAAT/enhancer binding protein (C/EBP) family of transcription factors [12]. C/EBP- β is induced in the early phase of adipogenesis and is crucial for activating PPAR γ expression. PPAR γ collaborates with C/EBP- α to bind and regulate the expression of most adipocyte-associated genes, including *aP2*, in fat cells [13]. Many transcription factors that direct cells toward a brown/beige adipocyte identity rather than a white adipocyte identity act by modulating the core adipogenic transcriptional machinery. PRDM16, which is one of the most important transcriptional co-regulators of brown/beige adipocyte differentiation [14], promotes a brown fat-selective gene program, mainly via protein-protein interactions with transcriptional factors such as C/EBP- β , PPAR γ , and zinc finger protein 516 (Zfp516) [3,15,16].

Zinc is an essential nutrient for all living organisms and is required for the structure and function of a wide range of proteins; 10% of all human proteins have the potential to bind zinc [17]. Zinc acts as both an intracellular and extracellular signaling effector; zinc signaling is mediated by zinc transporters and metallothioneins that regulate various cellular functions [18]. Cellular zinc homeostasis is tightly regulated by two families of zinc transporter proteins, namely, the zinc transporter (ZnT) family, which controls zinc efflux out of the cytosol, and the Zrt/Irt-related protein (ZIP) family, which controls zinc influx into the cytosol [19]. Dysfunction of zinc signaling leads to physiological disturbances. For example, our group and others showed that extracellular zinc signaling via the zinc transporter ZnT8 regulates hepatic insulin clearance, and that altered ZnT8 function is involved in type 2 diabetes pathogenesis [20,21], indicating that the precise control of zinc homeostasis is crucial for maintaining health and preventing diseases, including lifestyle-associated diseases. Intriguingly, zinc deficiency significantly reduces the DNA-binding activity of PPARs [22], suggesting that some zinc-containing proteins that participate in brown/beige adipocyte differentiation and function (e.g., PRDM16, Kruppel-like factor 11 (KLF11), and *Zfp516*) might be dysregulated by changes in zinc homeostasis.

In this study, we focused on the zinc transporter ZIP13 because *Zip13*-deficient (*Zip13*-KO) mice and humans with spondylocheirodysplastic Ehlers-Danlos syndrome who carry a loss-of-function mutation in *SLC39A13* have been reported to have a significantly decreased white fat mass [23]. We show that ZIP13 is a crucial regulator of beige adipocyte differentiation, and negatively regulates C/EBP- β protein levels, illustrating the physiological relevance of the ZIP13-C/EBP- β axis in beige adipocyte biogenesis and thermogenesis, and its therapeutic potential in obesity treatment.

Results

Inguinal fat tissue browning is accelerated in *Zip13*-KO mice

We previously reported that ZIP13 may be involved in adipose tissue homeostasis [23]. To clarify this point, we first weighed the WAT and BAT of *Zip13*-KO mice and their wild-type (WT) littermates (control). As shown in [S1A Fig](#), the interscapular BAT and inguinal WAT (iWAT) weights were similar in *Zip13*-KO and WT mice, but the epididymal WAT (eWAT) weight was significantly lower in *Zip13*-KO mice. *Zip13* expression was higher in the eWAT and BAT than in the iWAT ([S1B Fig](#)). Surprisingly, hematoxylin and eosin (H & E) staining of the iWAT in *Zip13*-KO mice showed large clusters of cells with multilocular lipid droplets, which are characteristic of the browning of iWAT depots ([Fig 1A](#)). Consistently, immunohistochemical staining revealed a high number of UCP1-positive cells in the *Zip13*-KO iWAT ([Fig 1B](#)); gene expression analyses confirmed that brown fat genes were significantly upregulated in the *Zip13*-KO iWAT ([Fig 1C](#)). There were no significant differences between WT and *Zip13*-KO mice in eWAT and BAT morphology, or in the expression of various brown adipocyte markers in BAT ([Fig 1A and 1D](#), [S1C Fig](#)); however, we observed that the expression of brown adipocyte markers in the eWAT of *Zip13*-KO mice tended to be higher than that of WT mice, although statistical significance was not observed ([S1D Fig](#)).

We assessed overall gene expression changes in the iWAT by microarray analyses of RNAs isolated from the iWATs of *Zip13*-KO mice and their WT littermates, and identified differentially expressed genes (1,260 upregulated and 1,082 downregulated genes in *Zip13*-KO mice compared with WT mice) ([S2A Fig](#) and [S1 Table](#)). Gene Ontology Biological Process (GOBP) analysis and Kyoto Encyclopedia of Genes and Genomes (KEGG) pathway enrichment analysis revealed that genes involved in inflammatory responses were downregulated, whereas genes involved in fatty acid metabolism and mitochondrial function were upregulated in the

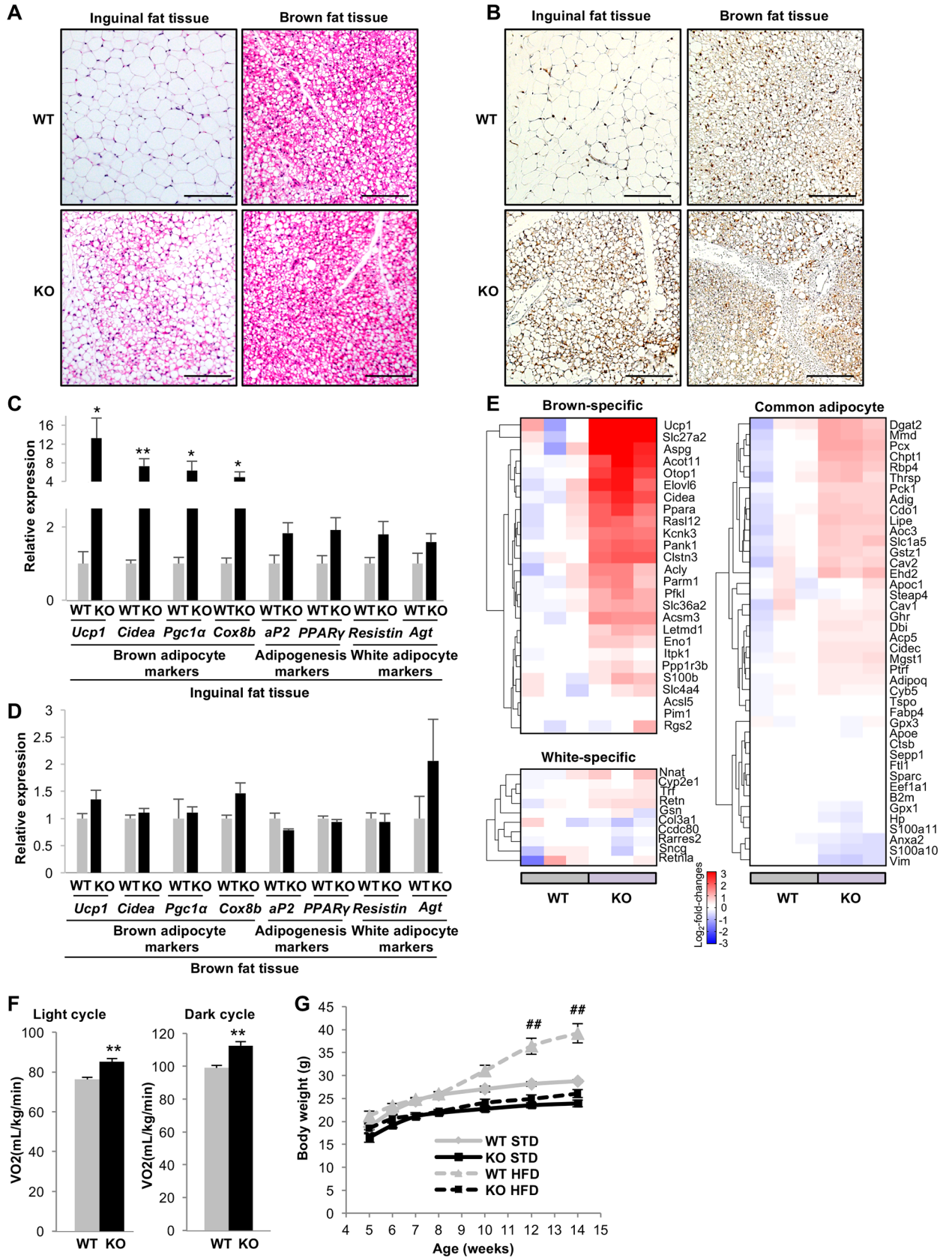


Fig 1. Upregulation of inguinal fat tissue browning and O₂ consumption rate in *Zip13*-KO mice. (A) H & E staining of inguinal fat and brown fat tissue in 10-week-old WT and *Zip13*-KO mice. Scale bars = 100 μm. (B) Immunohistochemical staining of the UCP1 in inguinal fat and brown fat tissue sections from 10-week-old WT and *Zip13*-KO mice. Scale bars = 100 μm. (C) Expression of the indicated genes in the inguinal fat tissue of 10-week-old WT and *Zip13*-KO mice (n = 5–6). (D) Expression of the indicated genes in the brown fat tissue of 10-week-old WT and *Zip13*-KO mice (n = 5–6). (E) Heat map of mRNA levels of brown fat-specific, white fat-specific, and common fat genes in the iWAT from 10-week-old WT and *Zip13*-KO mice (n = 3). (F) Energy expenditure of 10-week-old WT and *Zip13*-KO mice during the light (left) or dark cycle (right) (n = 4–6). (G) Body weights of mice from 5 to 14 weeks of age when fed a standard (STD) or high-fat diet (HFD) (n = 7–9). Error bars show SEM. **p* < 0.05, ***p* < 0.01 (WT vs. *Zip13*-KO), ###*p* < 0.01 (WT STD vs. WT HFD).

<https://doi.org/10.1371/journal.pgen.1006950.g001>

Zip13-KO iWAT, suggesting that an accelerated adipocyte-browning process occurs in the iWAT of *Zip13*-KO mice (S2B and S2C Fig, S2 Table). Pan et al. identified brown fat-specific, white fat-specific, and common fat genes by the RNA-sequencing of BAT, eWAT, and soleus-muscle tissue [24]. We used these criteria to profile the gene expression patterns in the *Zip13*-KO iWAT, and demonstrated the upregulation of a broad spectrum of brown fat-specific genes, a slight upregulation in common fat genes, and no change in white fat-specific genes (Fig 1E). Furthermore, the oxygen consumption rate (OCR) was significantly higher in the inguinal fat tissue of *Zip13*-KO mice than that of WT mice (S1E Fig), although there was no significant difference of OCR in brown fat tissue between the two groups. These results indicate that there was an increase in the number of functional beige adipocytes in *Zip13*-KO inguinal fat tissue.

O₂ consumption rate is elevated in *Zip13*-KO mice

The increase in beige adipocyte characteristics in *Zip13*-KO mice prompted us to examine the metabolic profiles of these mice. Indeed, we observed a significantly higher oxygen consumption (VO₂) rate in *Zip13*-KO mice than in WT mice under both light and dark conditions at 23°C (Fig 1F), without any changes in food intake (S3A Fig). Furthermore, the locomotor activity of the *Zip13*-KO mice tended to decrease (S3B Fig), although this change was not statistically significant. These results suggested that the increase in VO₂ in *Zip13*-KO mice was not due to hyperactivity or impaired food intake. To further investigate the role of ZIP13 in thermogenesis, we measured VO₂ in thermoneutral conditions (30°C) after activation of the β₃-adrenoreceptor agonist [25]. As shown in S3C Fig, VO₂ levels of *Zip13*-KO mice were significantly increased after the administration of β₃-adrenoreceptor agonist CL316,243, suggesting that ZIP13 might play a role in thermogenesis. We subsequently examined whether *Zip13*-KO mice acquired resistance to high-fat diet (HFD)-induced obesity. Body weights of WT mice were significantly increased by the HFD compared with a standard diet (STD); however, *Zip13*-KO mice were resistant to HFD-induced obesity primarily due to low fat mass gain (Fig 1G, S4A and S5A–S5E Figs). Furthermore, *Zip13*-KO mice appeared to have an improved glucose tolerance and insulin tolerance, compared to WT mice (S4B and S5D Figs). Taken together, these results indicated that *Zip13* deletion *in vivo* promotes beige adipocyte biogenesis and energy expenditure, and thereby reduces diet-induced obesity and insulin resistance.

ZIP13 negatively regulates adipocyte browning in a cell-autonomous manner

To clarify whether the increase in iWAT browning in *Zip13*-KO mice occurs in a cell-autonomous manner, primary white preadipocytes isolated from the iWAT of WT or *Zip13*-KO mice were cultured to induce their differentiation into adipocytes under defined conditions [26–28]. We found higher gene expression levels of several brown adipocyte markers and an adipogenesis marker (*aP2*) (Fig 2A and 2B), and higher total and oligomycin-insensitive cellular

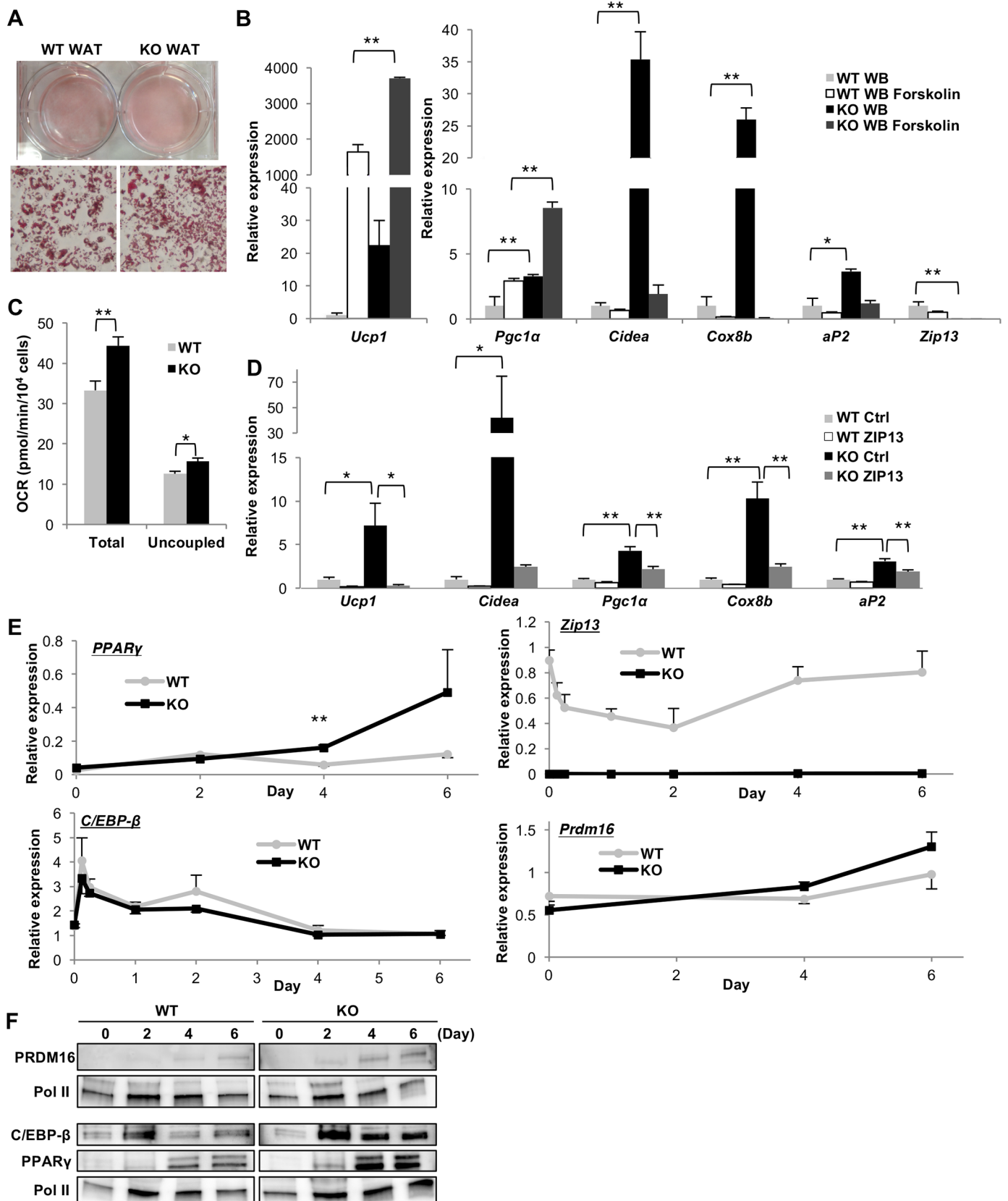


Fig 2. Adipocyte browning is accelerated in white preadipocytes from *Zip13*-KO mice. (A) Oil Red O staining of preadipocytes from WT and *Zip13*-KO mice in pro-adipogenic conditions. (B) Expression levels of the indicated genes in differentiated adipocytes in the presence or absence of forskolin ($n = 3$). (C) Total and uncoupled (oligomycin-insensitive) respiration of differentiated adipocytes ($n = 3$). (D) Differentiation of white preadipocytes from WT and *Zip13*-KO mice expressing an empty vector (Ctrl) or ZIP13-HA (ZIP13); mRNA levels of the indicated genes were measured using qRT-PCR ($n = 4$). (E) Time course of mRNA expression in differentiated white preadipocytes from WT and *Zip13*-KO mice ($n = 3$). (F) Time course of protein expression in WT and *Zip13*-KO preadipocytes after differentiation. Nuclear fractions were analyzed by immunoblotting. RNA Pol II was included as a loading control. Error bars show SEM. * $p < 0.05$, ** $p < 0.01$.

<https://doi.org/10.1371/journal.pgen.1006950.g002>

respiration in *Zip13*-KO cells than in WT cells (Fig 2C), suggesting that preadipocytes from *Zip13*-KO mice cell-autonomously accelerate adipocyte browning. Furthermore, treatment with the cAMP-inducer forskolin also increased the expression of thermogenic genes, including *Ucp1* and *Pgc1 α* , in *Zip13*-KO cells (Fig 2B), indicating that the differentiated cells were functional. Importantly, the exogenous expression of ZIP13 in *Zip13*-KO cells efficiently repressed the expression of brown adipocyte markers and the adipogenesis marker (Fig 2D, S6A Fig). Taken together, these results clearly demonstrate that ZIP13 negatively and cell-autonomously regulates adipocyte browning.

C/EBP- β protein levels are increased in *Zip13*-KO cells

To investigate the mechanism by which ZIP13 regulates adipocyte browning, we immortalized white preadipocytes from *Zip13*-KO and WT mice for further experiments. Stimulation with a cocktail that induces browning of adipocytes increased the expression of the adipogenic transcription factor PPAR γ in *Zip13*-KO cells (Fig 2E). Since PPAR γ is positively regulated by the transcription factors C/EBP- β and C/EBP- δ [29], we next examined C/EBP- β and C/EBP- δ gene and protein expression levels in these cells. Although the mRNA levels of C/EBP- β and C/EBP- δ genes were expressed comparably in *Zip13*-KO and WT cells (Fig 2E, S6B Fig), the C/EBP- β protein level in *Zip13*-KO cells was higher than that in WT cells at 2 days after inducing differentiation, before the upregulation of PPAR γ protein (Fig 2F). The expression of other early transcriptional regulators, such as *Krox20*, did not differ between WT and *Zip13*-KO cells (S6B Fig). C/EBP- β is not only important in adipogenesis, but is also essential for brown fat development; C/EBP- β cooperates with the coregulatory protein PRDM16 to act as a crucial molecular switch in determination of brown fat cell fate [15]. Intriguingly, PRDM16 protein levels also increased in *Zip13*-KO cells after 4 days of differentiation (Fig 2F), suggesting that ZIP13 is involved in the homeostatic regulation of C/EBP- β and the PRDM16 proteins, both of which are essential for adipocyte browning at either the post-transcriptional or translational level.

Zip13-KO cells resemble preadipocytes expressing high levels C/EBP- β protein

Since C/EBP- β is required in both white and brown adipocyte differentiation [12], we next investigated whether the regulatory expression of C/EBP- β in WT white preadipocytes might affect white versus beige adipocyte differentiation. When white preadipocytes stably expressing C/EBP- β (WPreC β cells) were differentiated using a cocktail that induces white adipocytes, several white adipocyte markers and the adipogenesis marker *aP2* were significantly increased (Fig 3A and 3B, S7, S8A and S8B Figs). However, this effect was due to the enhancement of adipogenesis *per se*, since white adipocyte marker genes were expressed at almost the same (or at a decreased) level between control and WPreC β cells when the mRNA levels of these genes were normalized to that of *aP2* (Fig 3C, S8C Fig). In contrast, when these cells were exposed to a brown adipogenic differentiation cocktail, brown adipocyte markers were significantly increased in WPreC β cells (Fig 3D, S8B Fig), and this was not likely to be due to enhanced

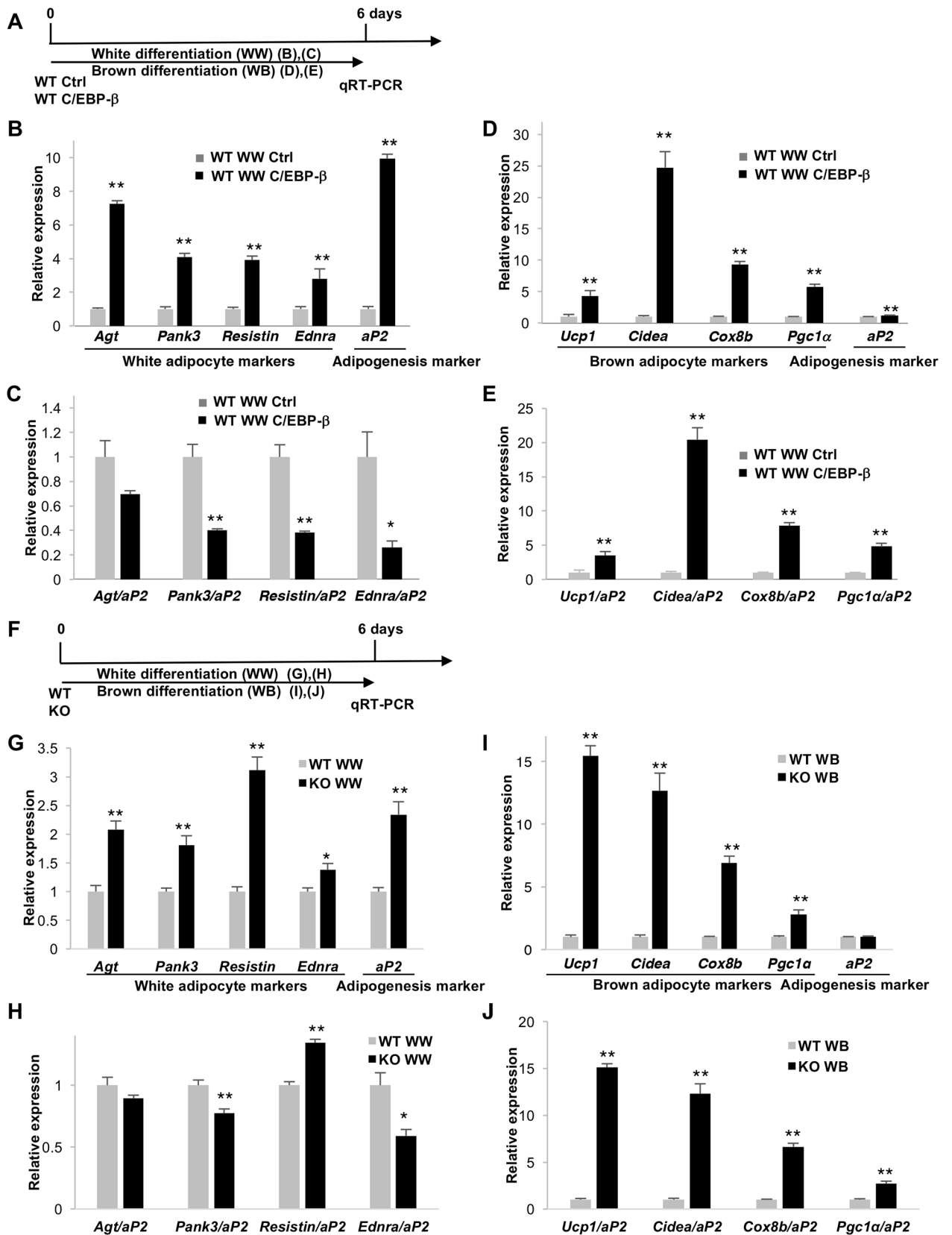


Fig 3. C/EBP- β overexpression accelerates adipocyte browning independently of adipogenesis. (A) Diagram showing the time course used in the following experiments (B-E) using WT white preadipocytes expressing a control vector (WT Ctrl) or HA-C/EBP- β (WT C/EBP- β). These cells were differentiated using a white adipogenic cocktail (WW) or a brown adipogenic cocktail (WB). (B) Expression of the indicated genes was measured by qRT-PCR ($n = 4$). (C) The mRNA levels of white adipocyte markers related to (B) were normalized to that of *aP2* ($n = 4$). (D) Expression levels of the indicated genes were measured by qRT-PCR ($n = 4$). (E) The mRNA levels of brown adipocyte markers related to (D) were normalized to that of *aP2* ($n = 4$). (F) Schematic of the time course used in (G-J) using WT (WT) and *Zip13*-KO (KO) white preadipocytes. (G) Expression of the indicated genes was measured using qRT-PCR ($n = 4$). (H) The mRNA levels for white adipocyte markers related to (G) were normalized to that of *aP2* ($n = 4$). (I) Expression of the indicated genes was measured using qRT-PCR ($n = 4$). (J) The mRNA levels of brown adipocyte markers related to (I) were normalized to that of *aP2* ($n = 4$). Error bars show SEM. * $p < 0.05$, ** $p < 0.01$.

<https://doi.org/10.1371/journal.pgen.1006950.g003>

adipogenesis, since this upregulation of brown adipocyte markers was still evident after normalizing the mRNA levels of these genes to those of *aP2* (Fig 3E, S8C Fig). These results indicate that C/EBP- β , an intrinsic transcription factor that positively regulates adipogenesis, facilitates beige adipocyte differentiation. These observations led us to further assess and compare the characteristics of *Zip13*-KO and WPreC β cells, since *Zip13*-KO cells accumulate the C/EBP- β protein (Fig 2F). In fact, we found that both white and brown adipocyte markers were increased in *Zip13*-KO cells (Fig 3F–3G and 3I, S8D and S8E Fig), and the enhanced expression of brown adipocyte markers in *Zip13*-KO cells was still evident when normalized to the expression of *aP2* (Fig 3H and 3J). Taken together, these results suggest that *Zip13*-KO cells have similar features to those of preadipocytes, which contain high levels of the C/EBP- β protein.

ZIP13-mediated C/EBP- β degradation pathway negatively regulates adipocyte browning

To further validate the intrinsic role of ZIP13 in adipocyte browning, we used C3H10T1/2 cells, which differentiate into brown/beige adipogenic lineages when exposed to a brown adipogenic cocktail. Depleting ZIP13 by RNAi significantly increased the expression of brown adipocyte markers (Fig 4A and 4B), which was further confirmed using another *Zip13* siRNA (S9A–S9D Fig). C/EBP- β protein levels were also increased by *Zip13* knockdown in C3H10T1/2 cells at the indicated time points (Fig 4C). The C/EBP- β protein level was investigated by a cycloheximide (CHX) chase experiment (Fig 4D and 4E), which suggested the possible involvement of ZIP13 in C/EBP- β protein stability.

We next investigated whether C/EBP- β ubiquitination was increased in *Zip13*-KO cells. Ubiquitinated C/EBP- β was detected by immunoprecipitation with the HA antibody, followed by immunoblotting with an anti-ubiquitin antibody. The level of ubiquitinated C/EBP- β protein was reduced by approximately half (0.48-fold decrease) in *Zip13*-KO cells compared with those in WT cells (Fig 4F), suggesting that C/EBP- β is resistant to ubiquitination in *Zip13*-KO cells, which might account for the increased adipocyte browning in these cells. To examine the biological relevance of C/EBP- β upregulation in *Zip13*-KO cells, we used retroviruses expressing short hairpin (sh) RNAs targeting C/EBP- β (sh β -1 and sh β -2) to downregulate C/EBP- β (Fig 4G), which efficiently blocked brown adipocyte differentiation (Fig 4H). These results indicated that the enhanced adipocyte browning due to loss of ZIP13 is caused by C/EBP- β accumulation.

ZIP13-mediated zinc transport negatively regulates adipocyte browning

We next investigated whether the zinc-transporting activity of ZIP13 is necessary for moderate adipocyte browning. The most highly conserved portions among the ZIP-family proteins are reported to be in transmembrane domains (TMDs) IV and V, which both contain common

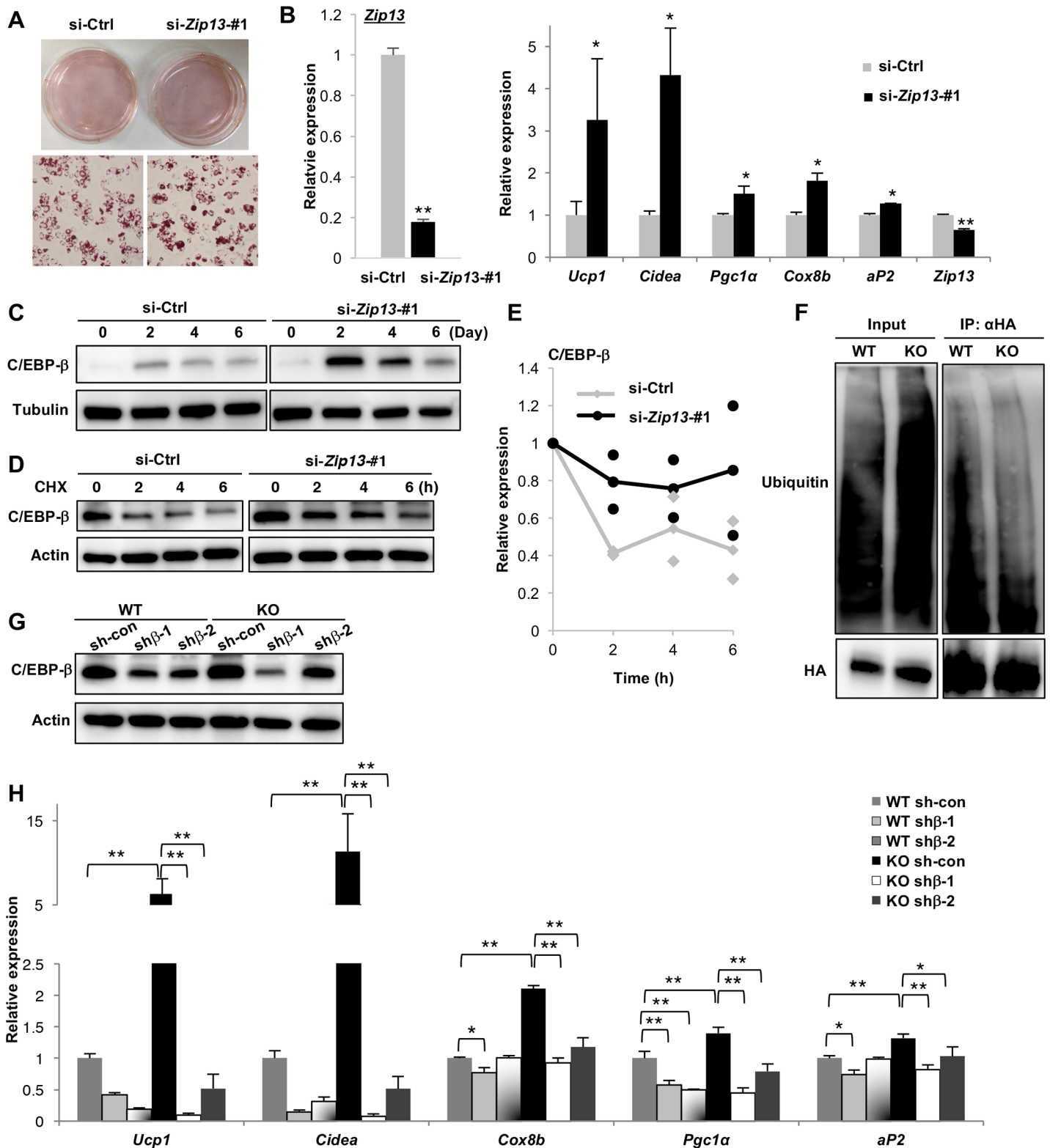


Fig 4. ZIP13 negatively regulates adipocyte browning by stabilizing C/EBP-β. (A) C3H10T1/2 cells transfected with an siRNA targeting *Zip13* (si-*Zip13*-#1) or a non-targeting control (si-Ctrl) were stained with Oil Red O after induction of adipocyte differentiation. (B) Left panel: *Zip13* expression after the 2.5 days of transfection; Right panel: Expression of the indicated genes was measured using qRT-PCR (n = 4). (C) Protein expression of C/EBP-β. Tubulin was used as a loading control. (D) Protein expression of C/EBP-β in the presence of CHX. C3H10T1/2 cells were transfected with the si-*Zip13*-#1

or si-Ctrl oligonucleotide; β -actin is shown as a loading control. (E) C/EBP- β protein levels were quantified by normalization to the protein level at 0 h. Each dot shows two independent experiment results and lines show the average of the experiments. (F) HA-C/EBP- β immunoprecipitation, followed by immunoblotting to detect ubiquitin. (G) Protein expression of C/EBP- β in WT and *Zip13*-KO preadipocytes expressing scramble control (sh-con) or shRNA targeting C/EBP- β (sh β -1, or sh β -2); β -actin is shown as a loading control. (H) Expression of the indicated genes, measured by qRT-PCR (n = 4). Error bars show SEM. * p < 0.05, ** p < 0.01.

<https://doi.org/10.1371/journal.pgen.1006950.g004>

amino acids required for zinc binding, such as His (Fig 5A) [30]. To address whether these residues of ZIP13 contribute to intracellular zinc homeostasis, we generated a series of ZIP13 mutants (H229A and H254A) in which the His residues were replaced with Ala in TMDs IV and V (Fig 5B). As shown in Fig 5C, cells with exogenous expression of ZIP13 (WT) showed significantly upregulated *MT1A* mRNA levels, which correlates with cytosolic zinc levels, compared to the control (Ctrl); this result is consistent with previous reports [31,32] (Fig 5C). In contrast, exogenous expression of H229A or H254A mutant ZIP13 decreased the mRNA level of *MT1A* compared with ZIP13 (WT) (Fig 5C). Homophilic interactions (Fig 5D) and intracellular localization of these mutants were similar to those in the WT (Fig 5E), as previously reported [31]. Together, these findings indicated that H229 and H254 are important for increasing cytosolic zinc levels.

We next ectopically expressed the loss-of-function ZIP13 mutants in *Zip13*-KO cells in rescue experiments to determine whether they suppress the adipocyte browning induced by ZIP13 deficiency. Interestingly, expression of these loss-of-function ZIP13 mutants (H229A or H254A) could not suppress the adipocyte-browning phenotype (Fig 5F) or decrease C/EBP- β protein levels in *Zip13*-KO cells (Fig 5G). Finally, we examined whether zinc ion treatment could rescue the adipocyte-browning phenotype of *Zip13*-KO cells. Exogenous zinc ion treatment increased *MT1A* levels (S10A and S10B Fig) but did not reverse the adipocyte browning induced by ZIP13 deficiency (S10C Fig), indicating that specific zinc transport mediated by ZIP13 is indispensable for the proper homeostasis of adipocyte browning.

Discussion

ZIP13 is necessary for proper beige adipocyte differentiation in a cell-autonomous manner

The iWAT in *Zip13*-KO mice showed a browning phenotype that reflected increased energy expenditure (Fig 1A–1C and 1F, S1E Fig). Gene expression profiling showed that common fat genes were slightly upregulated in the iWAT of *Zip13*-KO mice, the expression of brown fat-specific genes were more notably increased, and the expression of white fat-specific genes was minimally affected (Fig 1E). These unbiased analyses demonstrated that ZIP13 is unlikely to be involved in the fate decision of white versus beige fat, but is likely involved in the inhibition of beige fat differentiation.

The differentiation of mesenchymal stem cells into adipocytes is regulated by a series of transcription factors that determine the sequence of events, such as commitment, differentiation, and activation [1]. For example, BMP7 and EBF2 are crucial for mesenchymal progenitor cells to commit to a brown or beige fat lineage [33,34]. Therefore, if these factors are activated in *Zip13*-KO cells, the expression of adipogenic regulators (such as C/EBP- β , C/EBP- δ , and *Krox20*) at the early stages should be upregulated. However, there was no change in the expression of these genes between WT and *Zip13*-KO cells (Fig 2E, S6B Fig). Instead, C/EBP- β protein levels were increased in *Zip13*-KO cells (Fig 2F), causing accelerated beige adipocyte differentiation. Exposure to cold, norepinephrine, or forskolin activates brown/beige adipocytes to express high levels of thermogenic genes [1]. In fact, we found that *Zip13*-KO cells exhibited increased thermogenic gene expression upon exposure to forskolin (Fig 2B),

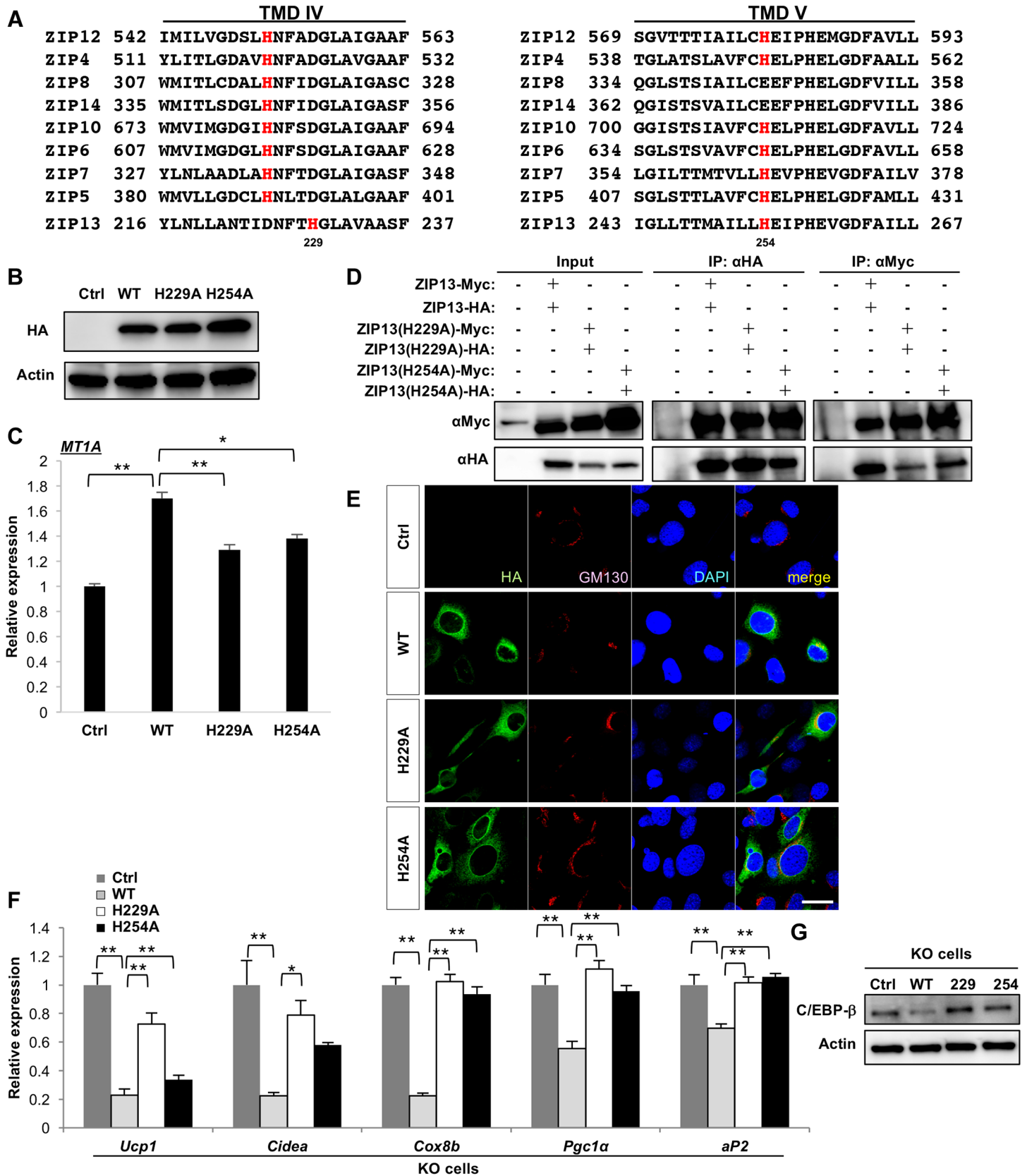


Fig 5. ZIP13-mediated zinc flux negatively regulates adipocyte browning. (A) Amino acid alignment of TMD IV and V among selected members of the mouse ZIP family. The His residues in TMD IV and V (red) are putative zinc-binding sites that are highly conserved among ZIP-family members. (B) Expression of WT ZIP13 and ZIP13 mutants (H229A and H254A) in C3H10T1/2 cells; β -actin is shown as a loading control. (C) *MT1A* gene expression in C3H10T1/2 cells expressing WT and mutant (H229A and H254A) ZIP13 ($n = 4$). We have showed the results that appeared to be statistically significant against the WT background. (D) Immunoprecipitation of HA- or Myc-tagged WT, H229A, or H254A ZIP13, followed by immunoblotting for HA- or Myc-tagged ZIP13 to detect the homophilic characteristics of the ZIP13 mutants H229A and H254A. (E) Subcellular localization of ZIP13-HA (WT, H229A, or H254A) expressed in *Zip13*-KO preadipocytes. Cells expressing HA-tagged WT, H229A, or H254A ZIP13 (left panels) were double-stained with the Golgi apparatus marker GM130 (middle panels); the merged images are shown on the right. Scale bars = 40 μ m. (F) Expression levels of the indicated genes in *Zip13*-KO cells expressing Ctrl, WT ZIP13, or the H229A or H254A ZIP13 mutant ($n = 4$). (G) Expression of C/EBP- β protein 4 days after differentiation; β -actin is shown as a loading control. Error bars show SEM. * $p < 0.05$, ** $p < 0.01$.

<https://doi.org/10.1371/journal.pgen.1006950.g005>

indicating that functional beige adipocytes are increased. However, the rate of increase in thermogenic gene expression was similar between *Zip13*-KO and WT cells (Fig 2B). These results suggested that ZIP13 is mainly involved in the differentiation rather than the activation of beige adipocytes.

We demonstrated that preadipocytes from *Zip13*-KO mice accelerate adipocyte browning at a higher rate than those from WT mice (Fig 2A–2C), and *Zip13* knockdown experiments showed similar results (Fig 4A and 4B). Furthermore, the exogenous expression of ZIP13 in *Zip13*-KO cells efficiently repressed adipocyte browning (Fig 2D). These results suggest that ZIP13 negatively regulates adipocyte browning in a cell-autonomous manner. We also showed that functional beige fat cells were increased in inguinal fat tissue of *Zip13*-KO mice (Fig 1A and 1C, S1E Fig), which might contribute to an increase in whole body VO_2 of *Zip13*-KO mice (Fig 1F). Furthermore, the observation that the β 3-adrenoreceptor agonist treatment increased whole-body energy expenditure even under thermoneutrality, indicated that beige fat of *Zip13*-KO mice at least partially contributed to the whole-body energy expenditure even if *Zip13*-KO mice were global KO mice. However, we cannot rule out the possibility that tissues other than beige fat might contribute to the increased in whole-body VO_2 of *Zip13*-KO mice since *Zip13*-KO mice do have dermal defects [35], and this could play an important role in the increase in beige fat activity, as reported by Cannon and Nedergaard [36]. Further investigation is necessary to test this possibility, by analyzing tissue-specific *Zip13*-KO mice.

ZIP13 is required for C/EBP- β homeostasis

C/EBP- β is involved in both adipogenesis and brown/beige adipocyte differentiation [12]. During adipogenesis, C/EBP- β induces the expression of C/EBP- α and PPAR γ , the two major transcriptional inducers of adipogenic gene expression. C/EBP- β -KO mice have severely impaired brown fat development and reduced *Ucp1* expression [37]. Overexpression of C/EBP- β induces *Ucp1* expression in 3T3-L1 white adipocytes [38]. Upstream activators of C/EBP- β induce brown/beige fat differentiation [26,39–41]. In fact, browning is accelerated not only in cultured white but also brown *Zip13*-KO adipocytes, and in brown fat tissue of *Zip13*-KO mice fed a HFD (Fig 2, S4D, S4F and S11 Figs). Furthermore, *Zip13* knockdown increased adipocyte browning in C3H10T1/2 cells, which are capable of differentiating into the beige or brown adipocyte lineage when exposed to a brown adipogenic cocktail (Fig 4A–4C). These results suggest that *Zip13* may contribute to the browning of both white and brown adipocytes via the accumulation of C/EBP- β .

These findings raised the fundamental question of whether C/EBP- β stabilization provides a plausible explanation for the *Zip13* deficiency phenotype. We noted that white preadipocytes overexpressing C/EBP- β phenocopied *Zip13* deficiency with regard to accelerated adipocyte browning (Fig 3E and 3J, S8C and S8F Fig). Furthermore, the enhanced browning in *Zip13*-KO adipocytes was almost completely eliminated by C/EBP- β knockdown (Fig 4H). These results, obtained from overexpression or knockdown experiments, indicated that C/EBP- β stabilization is a crucial step for the enhanced browning resulting from ZIP13 deficiency.

An interesting observation in the present study was that C/EBP- β played specific roles in promoting beige adipocyte differentiation (Fig 3B–3E). C/EBP- β and PRDM16 comprise a transcriptional unit crucial for brown/beige fat differentiation; therefore, C/EBP- β protein induction might stabilize or recruit PRDM16 [42] and accelerate adipocyte browning. Indeed, PRDM16 expression was significantly increased in *Zip13*-KO cells compared with WT cells 4–6 days after the induction of differentiation (Fig 2F), supporting the idea that C/EBP- β protein accumulation stabilizes PRDM16.

ZIP13-mediated zinc transport regulates C/EBP- β protein levels

ZIP13 is shown to transport zinc from the Golgi apparatus to the cytoplasm in mammalian cells [23,43]. Thus, we investigated whether this zinc-transporting ability of ZIP13 is required for inhibiting adipocyte browning. The conserved His residues in the TMDs are required for zinc transport in other ZIP-family proteins [44], and we demonstrated that these His residues in ZIP13 were crucial for ZIP13-mediated zinc transport for the inhibition of adipocyte browning (Fig 5F–5G). One possible explanation is that zinc transport elicited by a specific zinc transporter contributes to the stability of a particular protein, hence enabling it to perform its physiological function.

C/EBP- β is regulated by several post-translational modifications that are crucial for proper activation of the adipogenic program, such as phosphorylation, ubiquitination, and sumoylation [45,46]. We showed that the amount of ubiquitinated C/EBP- β was decreased in *Zip13*-KO cells (Fig 4F), causing accelerated adipocyte browning. There are two possible mechanisms underlying this observation. The first is that the expression or activity of deubiquitinating enzymes is upregulated; the second is that the ubiquitin system is downregulated. In fact, zinc blocks the activity of these deubiquitinating enzymes, including cysteine protease [47], and zinc is required for the activity of ubiquitin system-related proteins, including the RING-finger family E3 ligase [48]. Therefore, the activity of these enzymes may be altered in *Zip13*-deficient cells. Further analysis of *Zip13*-deficient cells will clarify the specific roles of C/EBP- β in beige adipocyte differentiation.

We also demonstrated that ZIP13-mediated zinc transport, but not a sufficient zinc supply in the form of zinc ions, is required for stabilizing C/EBP- β (Fig 5G, S10 Fig), suggesting that ZIP13-mediated zinc transport plays a specific role in clearing C/EBP- β proteins to inhibit adipocyte browning. ZIP13-mediated zinc transport might specifically determine the molecular fate of C/EBP- β partners, such as deubiquitinating enzymes or the RING-finger family E3 ligase, thereby affecting C/EBP- β stability and the rate of adipocyte browning. These hypotheses should be further verified by identifying the binding partners of ZIP13 via proteomic studies.

In this study, while investigating the role of a causative gene for a human disease, we unexpectedly found a novel molecular adipocyte-browning mechanism regulated by the ZIP13-C/EBP- β signaling cascade (Fig 6). This system might be conserved in humans, considering the lean phenotype observed in a patient with a loss-of-function mutation of ZIP13 [23]. Elucidating the ZIP13-regulated adipocyte-browning pathway may contribute to the development of new therapeutics against obesity.

Methods

Animal studies

All mice were housed in specific pathogen-free barrier facilities, maintained under a 12-h light/dark cycle, given water *ad libitum*, and fed standard rodent feed (Oriental Yeast, Tokyo, Japan) or rodent feed containing 60% fat (Research Diet, New Brunswick, NJ, USA) from 8 to

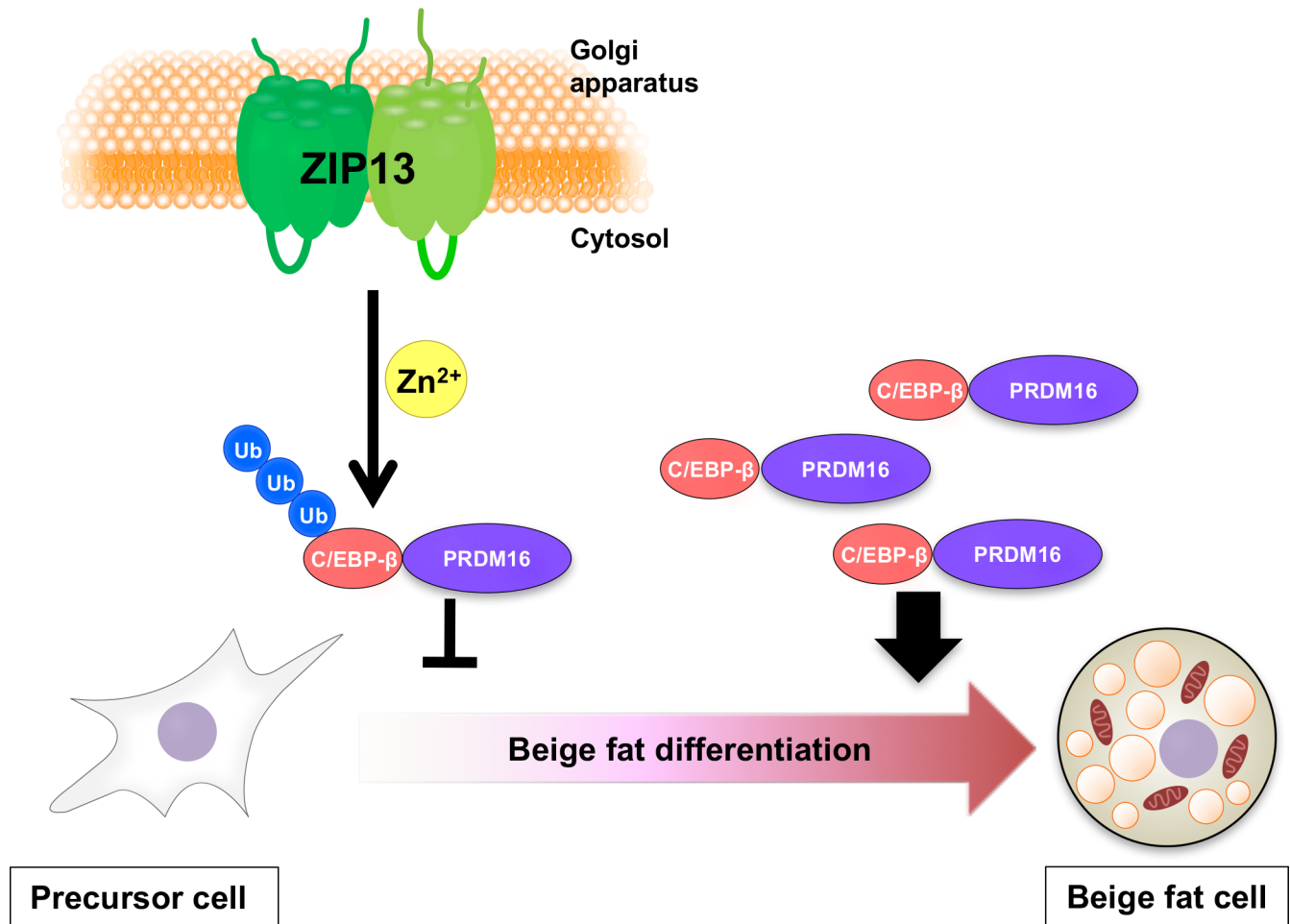


Fig 6. Schematic model of the role of ZIP13 in adipocyte browning. Zinc transport mediated by ZIP13 inhibits C/EBP-β accumulation, thereby negatively regulating adipocyte browning (left). Conversely, C/EBP-β accumulates in the *Zip13*-deficient condition (right).

<https://doi.org/10.1371/journal.pgen.1006950.g006>

14 weeks of age. As *Zip13*-KO mice show hypodontia [23], all mice used in the experiments were fed powdered feed to ensure adequate nutrition. All mice were backcrossed onto C57BL/6J mice for more than seven generations.

Metabolic studies

The whole-body energy expenditure of *Zip13*-KO or WT mice at 10 weeks of age was measured using an ARCO 2000 mass spectrometer (Arco System, Chiba, Japan).

Cell immortalization and culture

Immortalized white or brown preadipocytes were isolated from the iWAT or BAT of WT and *Zip13*-KO mice (6–8 weeks) by collagenase digestion, as described previously [49]. Preadipocytes were immortalized by retroviral transduction with the SV40T antigen and selection with puromycin (2 mg/mL). Immortalized preadipocytes were a mixed population and two cell lines were examined. Preadipocytes were seeded into collagen-coated dishes (Corning, Kennebunk, ME, USA) in DMEM/F12 (Gibco, Carlsbad, CA, USA) with 10% FCS. C3H10T1/2 cells were obtained from American Type Culture Collection. For white adipocyte differentiation,

cells were induced with induction medium containing 10% FBS, 5 $\mu\text{g}/\text{mL}$ insulin, 250 μM isobutylmethylxanthine (IBMX), and 2 $\mu\text{g}/\text{mL}$ dexamethasone in DMEM. Two days after induction, the culture medium was changed to a maintenance medium containing 10% FBS and 5 $\mu\text{g}/\text{mL}$ insulin. For the brown adipocyte cocktail, we used a formula described in previous reports [26–28]. Briefly, when the cells reached confluency, brown/beige adipocyte differentiation was induced by treating cells with DMEM containing 10% FBS, 250 μM IBMX, 2 $\mu\text{g}/\text{mL}$ dexamethasone, 125 μM indomethacin, 5 $\mu\text{g}/\text{mL}$ insulin, 1 nM T3, and 0.5 μM rosiglitazone. Two days after induction, the culture medium was changed to a maintenance medium containing 10% FBS, 5 $\mu\text{g}/\text{mL}$ insulin, 1 nM T3, and 0.5 μM rosiglitazone. For cAMP treatment, cells were incubated with 10 μM forskolin for 4 h.

RNAi-mediated gene knockdown

RNAi-mediated gene knockdown was performed as described previously [8]; siRNAs for *Zip13* were obtained from Invitrogen (Carlsbad, CA, USA) (silencer select siRNA [s206098] and stealth siRNA[MSS229105]).

Immunoblotting and immunoprecipitation experiments

Immunoblotting and immunoprecipitation were performed as described previously [50]. The following antibodies were used for immunoblotting: anti-C/EBP- β (1:1,000; Cell Signaling, Danvers, MA, USA), anti-PRDM16 (1:1,000) [51], anti-PPAR γ (1:1,000; Cell Signaling), anti-Rpb1CTD (RNA polymerase II CTD) (1:1000; Cell Signaling), anti-tubulin (1:3,000; Sigma-Aldrich, St Louis, MO, USA), or anti- β -actin (1:3,000; Sigma).

Gene expression analysis

Total RNA was isolated from tissues using QIAzol (Qiagen, Valencia, CA, USA) following the manufacturer's protocol. Reverse transcription reactions were performed using High Capacity cDNA Synthesis Kit (Applied Biosystems, Foster, CA, USA). The sequences of the primers used in this study are shown in S3 Table. Quantitative reverse transcriptase PCR (qRT-PCR) was performed with SYBR green fluorescent dye using an ABI 7500 Fast Real-Time PCR System. Relative mRNA expression was determined by relative standard curve methods using 18S as an internal control to normalize samples.

Microarray experiment

Samples were hybridized onto an array (Agilent SurePrint G3 Mouse GE 8x60K). The gene expression data set was deposited in the Gene Expression Omnibus database (GSE77933). Microarray analysis and functional enrichment analysis were as described in S1 Text.

Plasmid construction and virus production

C-terminally HA-tagged plasmids expressing mouse ZIP13 (mZIP13-HA) were constructed by inserting cDNA into a pcDNA3.1, pMX-IRES-GFP, or pBabe-puro vector. Plasmids expressing zinc transport-incompetent ZIP13 mutants were constructed using two-step PCR. The plasmid expressing HA-C/EBP- β was kindly provided by Dr. Y. Kido (Kobe University) [52]. All constructs were verified by sequencing. Phoenix packaging (PLAT-E) cells, provided by Dr. T. Kitamura (Tokyo University), were transfected with retroviral vectors by lipofection [53]. After 48 h, the viral supernatant was collected and filtered. Cells were incubated for 6 h with the viral supernatant supplemented with 10 $\mu\text{g}/\text{mL}$ polybrene.

Immunohistochemistry and immunocytochemistry

Immunohistochemical analysis was performed as described previously [20,54,55], using an anti-Ucp1 antibody (1:250 dilution, Abcam, St. Charles, MO, USA). Immunocytochemistry was performed as described previously [50]. Anti-HA (1:100; MBL, Nagoya, Japan) and anti-GM130 antibodies (1:250; Transduction Lab, Lexington, KY, USA) were used for staining.

Study approval

The protocol for animal experiments was approved by the Ethics Review Committee of Animal Experimentation of Juntendo University and Gunma University.

Statistical analysis

All quantitative data were reported as the mean \pm SEM. The Student's *t*-test was performed for the comparison of two groups. For multiple comparisons, analysis of variance was performed by Two-way ANOVA followed by Bonferroni's multiple comparison test or One-way ANOVA followed by Bonferroni's multiple comparison test. A *p*-value of less than 0.05 was considered to indicate a statistically significant difference between two groups.

Ethics statement

All mice were housed and cared for according to guidelines approved by the Animal Care and Use Committee of Juntendo University (280216), and by the Committee for Institutional Animal Care and Experimentation Committee at the Gunma University (16-048).

Supporting information

S1 Fig. Phenotype of adipose tissues in *Zip13*-KO mice. (A) Tissue weights of inguinal, epididymal, and brown fat tissues of WT and *Zip13*-KO mice. Tissue weights were normalized to whole-body weights. (B) The relative *Zip13* expression in various tissues from WT and *Zip13*-KO mice (*n* = 5–7). (C) H & E staining of epididymal fat in WT and *Zip13*-KO mice. Scale bars = 100 μ m. (D) Expression of the indicated genes in epididymal fat tissue (*n* = 5–7). (E) Oxygen consumption rate (OCR) of inguinal fat tissue and brown fat tissue of WT and *Zip13*-KO mice at 24–26 weeks of age (*n* = 3). Data are shown as the mean \pm SEM. **p* < 0.05, ***p* < 0.01.

(TIF)

S2 Fig. Characterization of upregulated or downregulated genes in *Zip13*-KO cells. (A) Genes that are upregulated or downregulated in *Zip13*-KO cells compared with WT cells. Color bar represents the gradient of log₂-fold-changes in each comparison. (B) Gene Ontology Biological Processes (GOBPs) represented by the genes upregulated or downregulated by *Zip13* deletion. GOBPs are represented by enrichment scores, $-\log_{10}(p)$, where *p* is the *p* value of the GOBPs that are enriched. (C) KEGG pathway enrichment represented by the genes upregulated or downregulated by *Zip13* deletion. The bars represent the enrichment scores, $-\log_{10}(p)$, where *p* is the *p* value.

(TIF)

S3 Fig. Metabolic phenotypes of *Zip13*-KO mice. (A) Average daily food intake of WT and *Zip13*-KO mice (*n* = 8–10). (B) Locomotor activity of WT and *Zip13*-KO at 18 weeks of age (*n* = 4–8). (C) Oxygen consumption rate of WT and *Zip13*-KO 10-week-old mice with CL316,243 (0.5mg/kg) under thermoneutral conditions (*n* = 5). Error bars are SEM. **p* < 0.05,

n.s., not significant.
(TIF)

S4 Fig. Phenotypes of *Zip13*-KO mice fed a HFD. (related to Fig 1) (A) Tissue weights of inguinal, epididymal, and brown fat tissues of WT and *Zip13*-KO mice after 6 weeks on a HFD. Tissue weights were normalized to whole-body weights. (B) Insulin tolerance testing (left and middle) and the cumulative area under the curve between 0 min and 60 min for ITT (right) of 16-week-old WT and *Zip13*-KO mice fed an HFD for 8 weeks ($n = 6-9$). (C) Fasting blood glucose (left) and fasting plasma insulin (right) levels of 15-week-old WT and *Zip13*-KO mice fed an HFD for 7 weeks ($n = 7-9$). (D) H & E staining of inguinal fat tissue and brown fat tissue in WT and *Zip13*-KO mice fed a HFD. Scale bars = 200 μm . (E) Expression of the indicated genes in inguinal fat tissue ($n = 6-7$). (F) Expression of the indicated genes in brown fat tissue ($n = 6-7$). Data are shown as the mean \pm SEM. * $p < 0.05$, ** $p < 0.01$.
(TIF)

S5 Fig. Phenotypes of *Zip13*-KO mice fed a HFD. (A) Body weights of mice from 5 to 9 weeks of age when fed a HFD ($n = 7-8$). (B) Lean mass (left) and Fat mass (right), (C) Lean mass/ Body weight (left) and Fat mass/Body weight (right) of WT and *Zip13*-KO mice fed an HFD for 6-7 weeks ($n = 7-8$). (D) CT evaluation of adiposity of WT and *Zip13*-KO mice after 6-7 weeks on a HFD. (E) CT evaluation of visceral fat mass and subcutaneous fat mass of WT and *Zip13*-KO mice after 6-7 weeks on a HFD. Tissue mass was normalized to whole-body weights. (F) Blood glucose concentrations were measured during the IPGTT in WT and *Zip13*-KO mice after 5-6 weeks on a HFD. Data are shown as the mean \pm SEM. * $p < 0.05$, ** $p < 0.01$.
(TIF)

S6 Fig. Expression of adipogenic regulators at the early stages. (A) Western blots demonstrating the retroviral expression of ZIP13-HA in WT and *Zip13*-KO white preadipocytes; β -actin is shown as a loading control. (B) Time course (0, 1, 4, 8, 24, and 48 h) of mRNA expression of the indicated genes in differentiated white preadipocytes derived from WT and *Zip13*-KO mice. Data are shown as the mean \pm SEM. * $p < 0.05$, ** $p < 0.01$.
(TIF)

S7 Fig. Expression of C/EBP- β . Western blot showing the stable HA-C/EBP- β expression in WT white preadipocytes; β -actin is shown as a loading control.
(TIF)

S8 Fig. C/EBP- β overexpression accelerates adipocyte browning independent of adipogenesis. (related to Fig 3) (A) Schematic representation of the time course used in the following studies (B and C). (B) Full panel of indicated genes (related to Fig 3B and 3D). (C) Full panel of indicated genes (related to Fig 3C and 3E). (D) Schematic representation of the time course used in the following studies (E and F). (E) Full panel of indicated genes (related to Fig 3G and 3I). (F) Full panel of indicated genes (related to Fig 3H and 3J). Data are shown as the mean \pm SEM. * $p < 0.05$, ** $p < 0.01$.
(TIF)

S9 Fig. *Zip13* knockdown increased adipocyte browning. (A) Diagram showing the time course of the experiments in B-D using C3H10T1/2 cells transfected with control siRNA (si-Ctrl) or *Zip13* siRNA (si-*Zip13*-#2). (B) *Zip13* expression decreased in C3H10T1/2 cells transfected with *Zip13* siRNA ($n = 3$). (C) Oil Red O staining of C3H10T1/2 cells transfected with si-Ctrl or si-*Zip13*-#2 under proadipogenic conditions. (D) The expression levels of the indicated genes were analyzed by qRT-PCR ($n = 4$). Data are shown as the mean \pm SEM. * $p < 0.05$,

** $p < 0.01$.
(TIF)

S10 Fig. Zinc ion could not rescue the browning phenotype of *Zip13*-KO cells. (A) Schematic showing the time course used in B and C. WT and *Zip13*-KO (KO) white preadipocytes were differentiated using a brown-adipogenic induction cocktail with or without 100 μ M ZnSO₄. (B) *MT1A* expression in WT and KO cells (n = 4). (C) Expression levels of the indicated genes were measured by qRT-PCR (n = 4). Data are shown as the mean \pm SEM. * $p < 0.05$, ** $p < 0.01$. Please note that the expression level of indicated genes of both KO cells and its zinc-treated cells were significantly increased compared to WT cells or its zinc-treated cells, respectively.

(TIF)

S11 Fig. ZIP13 negatively regulates brown adipocyte differentiation. (A) Expression of the indicated genes was measured by qRT-PCR (n = 4). (B) HA-tagged ZIP13 was expressed in *Zip13*-KO brown preadipocytes; β -actin was used as a loading control. (C) The brown preadipocytes derived from *Zip13*-KO mice expressing control (Ctrl) or HA-tagged ZIP13 (ZIP13) were differentiated. The mRNA expression levels of the indicated genes were measured by qRT-PCR (n = 4). (D) C/EBP- β protein expression at the indicated time points (0, 2, 4 and 6 days). WT and *Zip13*-KO brown preadipocytes were differentiated using a brown adipogenic cocktail at the indicated time points; Tubulin was shown as a loading control. Data are mean \pm SEM. * $p < 0.05$, ** $p < 0.01$.

(TIF)

S1 Table. Upregulated and downregulated genes in *Zip13*-KO mice.

(XLSX)

S2 Table. Gene Ontology Biological Process (GOBP) analysis and Kyoto Encyclopedia of Genes and Genomes (KEGG) pathway enrichment analysis.

(XLSX)

S3 Table. Primer sequences.

(PDF)

S1 Text. Supplemental methods.

(DOCX)

Acknowledgments

We thank Drs. T. Mita, K. Komiya, M. Tamaki, A. Popiel, T. Irie, K. Mishima, Juntendo University Research Administrator (JURA) and T. Saito for helpful suggestions, Drs. Y. Kido and T. Kitamura for providing materials, and N. Daimaru, E. Magoshi, K. Nakamura, S. Ishikawa, H. Tsujimura, Kurosawa, S. Ichinose, R. Kosuge, and GENOSTAFF for their excellent technical assistance. We also appreciate the assistance we received from the Mouse Facility and Cell Imaging Core, the Laboratory of Molecular and Biochemical Research, and the Research Support Center of Juntendo University.

Author Contributions

Conceptualization: Ayako Fukunaka, Toshiyuki Fukada, Yoshio Fujitani.

Data curation: Ayako Fukunaka.

Formal analysis: Ayako Fukunaka.

Funding acquisition: Ayako Fukunaka, Toshiyuki Fukada, Hirotaka Watada, Yoshio Fujitani.

Investigation: Ayako Fukunaka.

Methodology: Ayako Fukunaka, Jinhyuk Bhin, Takamasa Tsuzuki, Yuri Takamine, Bum-Ho Bin, Toshinori Yoshihara, Noriko Ichinoseki-Sekine, Hisashi Naito, Shinzaburo Takamiya, Tsutomu Sasaki, Takeshi Inagaki, Tadahiro Kitamura, Shingo Kajimura.

Project administration: Toshiyuki Fukada, Hirotaka Watada, Yoshio Fujitani.

Resources: Toshiyuki Fukada, Shingo Kajimura.

Supervision: Toshiyuki Fukada, Hirotaka Watada, Yoshio Fujitani.

Validation: Ayako Fukunaka, Luka Suzuki, Bum-Ho Bin, Takeshi Miyatsuka, Shinzaburo Takamiya, Tsutomu Sasaki, Takeshi Inagaki, Shingo Kajimura.

Writing – original draft: Ayako Fukunaka, Jinhyuk Bhin.

Writing – review & editing: Ayako Fukunaka, Toshiyuki Fukada, Shingo Kajimura, Hirotaka Watada, Yoshio Fujitani.

References

1. Kajimura S, Spiegelman BM, Seale P (2015) Brown and Beige Fat: Physiological Roles beyond Heat Generation. *Cell Metab* 22: 546–559. <https://doi.org/10.1016/j.cmet.2015.09.007> PMID: 26445512
2. Harms M, Seale P (2013) Brown and beige fat: development, function and therapeutic potential. *Nat Med* 19: 1252–1263. <https://doi.org/10.1038/nm.3361> PMID: 24100998
3. Ohno H, Shinoda K, Spiegelman BM, Kajimura S (2012) PPARgamma agonists induce a white-to-brown fat conversion through stabilization of PRDM16 protein. *Cell Metab* 15: 395–404. <https://doi.org/10.1016/j.cmet.2012.01.019> PMID: 22405074
4. Stanford KI, Middelbeek RJ, Townsend KL, An D, Nygaard EB, et al. (2013) Brown adipose tissue regulates glucose homeostasis and insulin sensitivity. *J Clin Invest* 123: 215–223. <https://doi.org/10.1172/JCI62308> PMID: 23221344
5. Seale P, Conroe HM, Estall J, Kajimura S, Frontini A, et al. (2011) Prdm16 determines the thermogenic program of subcutaneous white adipose tissue in mice. *J Clin Invest* 121: 96–105. <https://doi.org/10.1172/JCI44271> PMID: 21123942
6. Saito M, Okamatsu-Ogura Y, Matsushita M, Watanabe K, Yoneshiro T, et al. (2009) High incidence of metabolically active brown adipose tissue in healthy adult humans: effects of cold exposure and adiposity. *Diabetes* 58: 1526–1531. <https://doi.org/10.2337/db09-0530> PMID: 19401428
7. Berry DC, Jiang Y, Arpke RW, Close EL, Uchida A, et al. (2017) Cellular Aging Contributes to Failure of Cold-Induced Beige Adipocyte Formation in Old Mice and Humans. *Cell Metab* 25: 166–181. <https://doi.org/10.1016/j.cmet.2016.10.023> PMID: 27889388
8. Shinoda K, Luijten IH, Hasegawa Y, Hong H, Sonne SB, et al. (2015) Genetic and functional characterization of clonally derived adult human brown adipocytes. *Nat Med* 21: 389–394. <https://doi.org/10.1038/nm.3819> PMID: 25774848
9. Sidossis L, Kajimura S (2015) Brown and beige fat in humans: thermogenic adipocytes that control energy and glucose homeostasis. *J Clin Invest* 125: 478–486. <https://doi.org/10.1172/JCI78362> PMID: 25642708
10. Yoneshiro T, Aita S, Matsushita M, Kayahara T, Kameya T, et al. (2013) Recruited brown adipose tissue as an antiobesity agent in humans. *J Clin Invest* 123: 3404–3408. <https://doi.org/10.1172/JCI67803> PMID: 23867622
11. Lee P, Smith S, Linderman J, Courville AB, Brychta RJ, et al. (2014) Temperature-acclimated brown adipose tissue modulates insulin sensitivity in humans. *Diabetes* 63: 3686–3698. <https://doi.org/10.2337/db14-0513> PMID: 24954193
12. Guo L, Li X, Tang QQ (2015) Transcriptional regulation of adipocyte differentiation: a central role for CCAAT/enhancer-binding protein (C/EBP) beta. *J Biol Chem* 290: 755–761. <https://doi.org/10.1074/jbc.R114.619957> PMID: 25451943
13. Tang QQ, Lane MD (2012) Adipogenesis: from stem cell to adipocyte. *Annu Rev Biochem* 81: 715–736. <https://doi.org/10.1146/annurev-biochem-052110-115718> PMID: 22463691

14. Seale P, Kajimura S, Yang W, Chin S, Rohas LM, et al. (2007) Transcriptional control of brown fat determination by PRDM16. *Cell Metab* 6: 38–54. <https://doi.org/10.1016/j.cmet.2007.06.001> PMID: 17618855
15. Kajimura S, Seale P, Kubota K, Lunsford E, Frangioni JV, et al. (2009) Initiation of myoblast to brown fat switch by a PRDM16-C/EBP-beta transcriptional complex. *Nature* 460: 1154–1158. <https://doi.org/10.1038/nature08262> PMID: 19641492
16. Dempersmier J, Sambeat A, Gulyaeva O, Paul SM, Hudak CS, et al. (2015) Cold-inducible Zfp516 activates UCP1 transcription to promote browning of white fat and development of brown fat. *Mol Cell* 57: 235–246. <https://doi.org/10.1016/j.molcel.2014.12.005> PMID: 25578880
17. Andreini C, Banci L, Bertini I, Rosato A (2006) Zinc through the three domains of life. *J Proteome Res* 5: 3173–3178. <https://doi.org/10.1021/pr0603699> PMID: 17081069
18. Spahl DU, Berendji-Grun D, Suschek CV, Kolb-Bachofen V, Kroncke KD (2003) Regulation of zinc homeostasis by inducible NO synthase-derived NO: nuclear metallothionein translocation and intracellular Zn²⁺ release. *Proc Natl Acad Sci U S A* 100: 13952–13957. <https://doi.org/10.1073/pnas.2335190100> PMID: 14617770
19. Hara T, Takeda TA, Takagishi T, Fukue K, Kambe T, et al. (2017) Physiological roles of zinc transporters: molecular and genetic importance in zinc homeostasis. *J Physiol Sci* 67: 283–301. <https://doi.org/10.1007/s12576-017-0521-4> PMID: 28130681
20. Tamaki M, Fujitani Y, Hara A, Uchida T, Tamura Y, et al. (2013) The diabetes-susceptible gene SLC30A8/ZnT8 regulates hepatic insulin clearance. *J Clin Invest* 123: 4513–4524. <https://doi.org/10.1172/JCI68807> PMID: 24051378
21. Flannick J, Thorleifsson G, Beer NL, Jacobs SB, Grarup N, et al. (2014) Loss-of-function mutations in SLC30A8 protect against type 2 diabetes. *Nat Genet* 46: 357–363. <https://doi.org/10.1038/ng.2915> PMID: 24584071
22. Reiterer G, MacDonald R, Browning JD, Morrow J, Matveev SV, et al. (2005) Zinc deficiency increases plasma lipids and atherosclerotic markers in LDL-receptor-deficient mice. *J Nutr* 135: 2114–2118. PMID: 16140885
23. Fukada T, Civic N, Furuichi T, Shimoda S, Mishima K, et al. (2008) The zinc transporter SLC39A13/ZIP13 is required for connective tissue development; its involvement in BMP/TGF-beta signaling pathways. *PLoS One* 3: e3642. <https://doi.org/10.1371/journal.pone.0003642> PMID: 18985159
24. Pan D, Huang L, Zhu LJ, Zou T, Ou J, et al. (2015) Jmjd3-Mediated H3K27me3 Dynamics Orchestrate Brown Fat Development and Regulate White Fat Plasticity. *Dev Cell* 35: 568–583. <https://doi.org/10.1016/j.devcel.2015.11.002> PMID: 26625958
25. Feldmann HM, Golozoubova V, Cannon B, Nedergaard J (2009) UCP1 ablation induces obesity and abolishes diet-induced thermogenesis in mice exempt from thermal stress by living at thermoneutrality. *Cell Metab* 9: 203–209. <https://doi.org/10.1016/j.cmet.2008.12.014> PMID: 19187776
26. Shan T, Xiong Y, Zhang P, Li Z, Jiang Q, et al. (2016) Lkb1 controls brown adipose tissue growth and thermogenesis by regulating the intracellular localization of CRTC3. *Nat Commun* 7: 12205. <https://doi.org/10.1038/ncomms12205> PMID: 27461402
27. Altshuler-Keylin S, Shinoda K, Hasegawa Y, Ikeda K, Hong H, et al. (2016) Beige Adipocyte Maintenance Is Regulated by Autophagy-Induced Mitochondrial Clearance. *Cell Metab* 24: 402–419. <https://doi.org/10.1016/j.cmet.2016.08.002> PMID: 27568548
28. Zhu Q, Ghoshal S, Rodrigues A, Gao S, Asterian A, et al. (2016) Adipocyte-specific deletion of Irf6k1 reduces diet-induced obesity by enhancing AMPK-mediated thermogenesis. *J Clin Invest* 126: 4273–4288. <https://doi.org/10.1172/JCI85510> PMID: 27701146
29. Park JH, Kang HJ, Kang SI, Lee JE, Hur J, et al. (2013) A multifunctional protein, EWS, is essential for early brown fat lineage determination. *Dev Cell* 26: 393–404. <https://doi.org/10.1016/j.devcel.2013.07.002> PMID: 23987512
30. Kambe T, Tsuji T, Hashimoto A, Isumura N (2015) The Physiological, Biochemical, and Molecular Roles of Zinc Transporters in Zinc Homeostasis and Metabolism. *Physiol Rev* 95: 749–784. <https://doi.org/10.1152/physrev.00035.2014> PMID: 26084690
31. Bin BH, Fukada T, Hosaka T, Yamasaki S, Ohashi W, et al. (2011) Biochemical characterization of human ZIP13 protein: a homo-dimerized zinc transporter involved in the spondylocheiro dysplastic Ehlers-Danlos syndrome. *J Biol Chem* 286: 40255–40265. <https://doi.org/10.1074/jbc.M111.256784> PMID: 21917916
32. Bin BH, Hojyo S, Hosaka T, Bhin J, Kano H, et al. (2014) Molecular pathogenesis of spondylocheirodysplastic Ehlers-Danlos syndrome caused by mutant ZIP13 proteins. *EMBO Mol Med* 6: 1028–1042. <https://doi.org/10.15252/emmm.201303809> PMID: 25007800

33. Tseng YH, Kokkotou E, Schulz TJ, Huang TL, Winnay JN, et al. (2008) New role of bone morphogenetic protein 7 in brown adipogenesis and energy expenditure. *Nature* 454: 1000–1004. <https://doi.org/10.1038/nature07221> PMID: 18719589
34. Wang W, Kissig M, Rajakumari S, Huang L, Lim HW, et al. (2014) Ebf2 is a selective marker of brown and beige adipogenic precursor cells. *Proc Natl Acad Sci U S A* 111: 14466–14471. <https://doi.org/10.1073/pnas.1412685111> PMID: 25197048
35. Hirose T, Ogura T, Tanaka K, Minaguchi J, Yamauchi T, et al. (2015) Comparative study of dermal components and plasma TGF-beta1 levels in Slc39a13/Zip13-KO mice. *J Vet Med Sci* 77: 1385–1389. <https://doi.org/10.1292/jvms.15-0015> PMID: 26050750
36. Nedergaard J, Cannon B (2014) The browning of white adipose tissue: some burning issues. *Cell Metab* 20: 396–407. <https://doi.org/10.1016/j.cmet.2014.07.005> PMID: 25127354
37. Tanaka T, Yoshida N, Kishimoto T, Akira S (1997) Defective adipocyte differentiation in mice lacking the C/EBPbeta and/or C/EBPdelta gene. *EMBO J* 16: 7432–7443. <https://doi.org/10.1093/emboj/16.24.7432> PMID: 9405372
38. Karamanlidis G, Karamitri A, Docherty K, Hazlerigg DG, Lomax MA (2007) C/EBPbeta reprograms white 3T3-L1 preadipocytes to a Brown adipocyte pattern of gene expression. *J Biol Chem* 282: 24660–24669. <https://doi.org/10.1074/jbc.M703101200> PMID: 17584738
39. Jimenez-Preitner M, Berney X, Uldry M, Vitali A, Cinti S, et al. (2011) Plac8 is an inducer of C/EBPbeta required for brown fat differentiation, thermoregulation, and control of body weight. *Cell Metab* 14: 658–670. <https://doi.org/10.1016/j.cmet.2011.08.008> PMID: 21982742
40. Mori M, Nakagami H, Rodriguez-Araujo G, Nimura K, Kaneda Y (2012) Essential role for miR-196a in brown adipogenesis of white fat progenitor cells. *PLoS Biol* 10: e1001314. <https://doi.org/10.1371/journal.pbio.1001314> PMID: 22545021
41. Chen Y, Siegel F, Kipschull S, Haas B, Frohlich H, et al. (2013) miR-155 regulates differentiation of brown and beige adipocytes via a bistable circuit. *Nat Commun* 4: 1769. <https://doi.org/10.1038/ncomms2742> PMID: 23612310
42. Harms MJ, Lim HW, Ho Y, Shapira SN, Ishibashi J, et al. (2015) PRDM16 binds MED1 and controls chromatin architecture to determine a brown fat transcriptional program. *Genes Dev* 29: 298–307. <https://doi.org/10.1101/gad.252734.114> PMID: 25644604
43. Jeong J, Walker JM, Wang F, Park JG, Palmer AE, et al. (2012) Promotion of vesicular zinc efflux by ZIP13 and its implications for spondylocheiro dysplastic Ehlers-Danlos syndrome. *Proc Natl Acad Sci U S A* 109: E3530–3538. <https://doi.org/10.1073/pnas.1211775110> PMID: 23213233
44. Antala S, Ovchinnikov S, Kamisetty H, Baker D, Dempsey RE (2015) Computation and Functional Studies Provide a Model for the Structure of the Zinc Transporter hZIP4. *J Biol Chem* 290: 17796–17805. <https://doi.org/10.1074/jbc.M114.617613> PMID: 25971965
45. Zhang YY, Li SF, Qian SW, Zhang YY, Liu Y, et al. (2012) Phosphorylation prevents C/EBPbeta from the calpain-dependent degradation. *Biochem Biophys Res Commun* 419: 550–555. <https://doi.org/10.1016/j.bbrc.2012.02.058> PMID: 22369944
46. Liu Y, Zhang YD, Guo L, Huang HY, Zhu H, et al. (2013) Protein inhibitor of activated STAT 1 (PIAS1) is identified as the SUMO E3 ligase of CCAAT/enhancer-binding protein beta (C/EBPbeta) during adipogenesis. *Mol Cell Biol* 33: 4606–4617. <https://doi.org/10.1128/MCB.00723-13> PMID: 24061474
47. Haase H, Maret W (2005) Protein tyrosine phosphatases as targets of the combined insulinomimetic effects of zinc and oxidants. *Biometals* 18: 333–338. <https://doi.org/10.1007/s10534-005-3707-9> PMID: 16158225
48. Budhidarmo R, Nakatani Y, Day CL (2012) RINGs hold the key to ubiquitin transfer. *Trends Biochem Sci* 37: 58–65. <https://doi.org/10.1016/j.tibs.2011.11.001> PMID: 22154517
49. Aune UL, Ruiz L, Kajimura S (2013) Isolation and differentiation of stromal vascular cells to beige/brite cells. *J Vis Exp* <https://doi.org/10.3791/50191> PMID: 23568137
50. Fukunaka A, Kurokawa Y, Teranishi F, Sekler I, Oda K, et al. (2011) Tissue nonspecific alkaline phosphatase is activated via a two-step mechanism by zinc transport complexes in the early secretory pathway. *J Biol Chem* 286: 16363–16373. <https://doi.org/10.1074/jbc.M111.227173> PMID: 21402707
51. Ohno H, Shinoda K, Ohyama K, Sharp LZ, Kajimura S (2013) EHMT1 controls brown adipose cell fate and thermogenesis through the PRDM16 complex. *Nature* 504: 163–167. <https://doi.org/10.1038/nature12652> PMID: 24196706
52. Matsuda T, Takahashi H, Mieda Y, Shimizu S, Kawamoto T, et al. (2015) Regulation of Pancreatic beta Cell Mass by Cross-Interaction between CCAAT Enhancer Binding Protein beta Induced by Endoplasmic Reticulum Stress and AMP-Activated Protein Kinase Activity. *PLoS One* 10: e0130757. <https://doi.org/10.1371/journal.pone.0130757> PMID: 26091000

53. Morita S, Kojima T, Kitamura T (2000) Plat-E: an efficient and stable system for transient packaging of retroviruses. *Gene Ther* 7: 1063–1066. <https://doi.org/10.1038/sj.gt.3301206> PMID: 10871756
54. Shigihara N, Fukunaka A, Hara A, Komiya K, Honda A, et al. (2014) Human IAPP-induced pancreatic beta cell toxicity and its regulation by autophagy. *J Clin Invest* 124: 3634–3644. <https://doi.org/10.1172/JCI69866> PMID: 25036706
55. Ebato C, Uchida T, Arakawa M, Komatsu M, Ueno T, et al. (2008) Autophagy is important in islet homeostasis and compensatory increase of beta cell mass in response to high-fat diet. *Cell Metab* 8: 325–332. <https://doi.org/10.1016/j.cmet.2008.08.009> PMID: 18840363